# Recent Development Trends in Materials for Bipolar Plates of Proton Exchange Membrane Fuel Cells (PEMFCs) and Kobe Steel's Activities

Toshiki SATO*1

*1 Materials Research Laboratory, Technical Development Group

**Abstract**

*Proton exchange membrane fuel cells (PEMFCs) are expected to become clean energy sources for transportation applications. Their bipolar plates, which are crucial parts of PEMFCs, significantly affect the durability, power-generation performance, and cost of PEMFCs. Thus, much effort has been made to improve the durability and performance of bipolar plates and reduce their costs. To improve the corrosion resistance and interfacial contact resistance (ICR), which affect the durability and characteristics of bipolar plates, Kobe Steel has been developing coated titanium using an unprecedented film and process since 2004. This paper reviews the recent development of carbon-polymer composites and coated metals, considered materials for bipolar plates, while focusing on their corrosion resistance and ICR. Also described is Kobe Steel's effort to develop film for titanium bipolar plates.*

## Introduction

Since the Industrial Revolution began in the mid-eighteenth century, the human race has produced various forms of energy by burning fossil fuels to enrich people's lives. On the other hand, greenhouse gases such as carbon dioxide, which are emitted into the atmosphere in large quantities as generative products, are causing global warming. This problem threatens the survival of the human race by driving up the average global temperature. Hence, efforts to achieve carbon neutrality, moving toward zero net greenhouse gas emissions, are rapidly accelerating worldwide. In Japan, the government declared in October 2020 that it aims to be carbon neutral by 2050.[1] Hydrogen plays a critical role in carbon neutrality. It is used for fuel cells, which are clean power generation systems that only emit water produced by the reaction of hydrogen and oxygen and essential products driving decarbonization. In particular, proton exchange membrane fuel cells (PEMFCs) have been used for automobiles,[5] thanks to their low-temperature operation, quick start, high energy efficiency, compact size, and light weight.[2-4] Their development is underway to reduce costs further and promote widespread use.

Among the components making up an automotive PEMFC, bipolar plates are estimated to account for 80% of the PEMFC's weight, 50-65% of its volume, and 35-40% of the PEMFC's total cost.[6] Since they are required to perform various functions, they are positioned as one of the essential components of PEMFCs, and efforts are being made to reduce costs and improve performance.

This paper reviews recent research and development trends in bipolar plates, which are vital components of automotive PEMFCs, focusing mainly on interfacial contact resistance (hereinafter referred to as "ICR") and durability, and also describes Kobe Steel's latest efforts in bipolar plate development.

## 1. PEMFC's structure and characteristics required for bipolar plate

**Fig. 1** schematically shows the structure of a PEMFC. A PEMFC comprises stacks of basic units called cells, surrounded by dotted squares. Each cell consists of a polymer electrolyte membrane coated with platinum catalyst on both sides and gas diffusion layers (hereinafter referred to as "GDLs") on both sides, which are sandwiched between bipolar plates from the outside. Conductive carbon paper or carbon cloth is used for the GDLs to distribute hydrogen and oxygen uniformly on the platinum catalyst surface and to conduct electrons. The power generation voltage per cell is approximately 0.6 to 1 V,[7-9] and to obtain high output, 300 to 400 cells are usually stacked for passenger car applications.[10, 11] Since two bipolar plates are required per cell, the number of bipolar plates_ranges from 600 to 800.

As shown in Fig. 1, a bipolar plate discharges water generated by flowing hydrogen and oxygen and also serves as a channel for cooling water flowing on the opposite side of the fuel gas. Therefore, channels must be formed on it by press forming or other means. The bipolar plate must also have high thermal conductivity because the cooling water plays a role in maintaining the PEMFC temperature at an appropriate level by removing the excess heat generated in the power generation process. In addition, since the bipolar plate serves as a current collector that collects and conducts

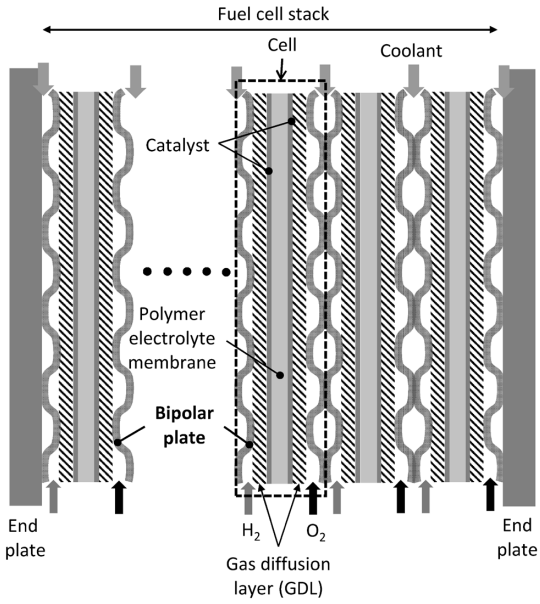


Fig. 1 Schematic diagram of a proton exchange membrane fuel cell (PEMFC) stack

Table 1 DOE technical targets for bipolar plates

| Characteristic | Units | 2025 target |
|---|---|---|
| Plate cost (guideline) | $/kW | 2 |
| Plate weight (guideline) | kg/kW | 0.18 |
| Plate $H_2$ permeation coefficient | Std $cm^3$ /sce·$cm^2$·Pa | $2\times10^{-6}$ @80°C, 3atm 100%RH |
| Corrosion anode (guideline) | μA/$cm^2$ | <1 and no active peak (pH3.0, 0.1ppmF, 80°C, Ar purge 0.1mV/s, -0.2 to 0.4VvsSHE |
| Corrosion cathode (guideline) | μA/$cm^2$ | <1 (pH3.0, 0.1ppmF, 80°C, aerated at 1.0VvsSHE for> 24h |
| Electrical conductivity | S/cm | >100 |
| Interfacial contact resistance | Ω·$cm^2$ | <0.01 (at a compaction force of 1.38MPa) |
| Flexural strength | MPa | >40 |
| Forming elongation | % | 40 |

electrons generated by the decomposition of hydrogen on the platinum catalyst, the resistance, or ICR, of the surface in contact with the GDL must be low. Furthermore, the inside of a PEMFC is a corrosive environment of acid with a pH of 2 to 3.[12), 13)] Thus, the bipolar plate is also required to have corrosion resistance. In the case of automotive applications, not only lightweight but also thinning of the bipolar plate is necessary because PEMFCs are often mounted in a limited space, for example, in passenger cars.[14)] They must also be strong enough to withstand automobiles' vibrations and mechanical shocks.[8)]

Thus, bipolar plates are required to have many functions and characteristics, as well as a low cost. As shown in **Table 1**, the US Department of Energy (hereinafter referred to as "DOE") has set 2025 target values for the cost and characteristics required for bipolar plates for transport equipment,[15)] and research and development are being conducted to achieve these target values. As a result of many research and development efforts, two promising materials have been identified: carbon-resin composite materials and surface-treated metals.

## 2. Bipolar plate materials

### 2.1 Carbon-resin composite material

A carbon-resin composite is a material in which a resin is mixed with more than a set amount of conductive carbon fillers to improve electrical conductivity by the phenomenon of rapid network formation among fillers based on the percolation theory[24)]. Those fillers include graphite powder,[16), 17)] expanded graphite powder,[16), 19), 20)] carbon fibers,[16)-18)] carbon black,[17), 18)] carbon nanotubes,[17), 18), 21)] and graphene.[22), 23)] Although its electrical conductivity, thermal conductivity, and material strength are inferior to those of metals, it has excellent corrosion resistance. Therefore, it has already been put into practical use in stationary fuel cells, where long-term durability is required, and there is little need to reduce size and weight through strength and thinning.[25)] In automotive applications, it is suitable for large commercial vehicles and buses with enough space for installation, even if the bipolar plate is thickened to ensure strength.[14), 26)]

The resin materials used as a base can be classified into two types: thermosetting resins such as phenol resin,[16), 19)] epoxy resin,[17), 18)] and vinyl ester resin;[28)] and thermoplastic resins such as polyethylene resin, polypropylene resin, polyphenylene sulfide resin,[20), 27)] polyvinylidene fluoride resin,[28), 29)] and polyphenylene sulfide resin.[30)] Thermosetting resins are cured by increasing the crosslink density through the polymerization reaction by heating and thus have high strength and heat resistance. It also has the advantage of being easy to increase electrical and thermal conductivity because it can be mixed with more carbon filler thanks to its low viscosity. On the other hand, it has the disadvantages of low toughness and low productivity compared with thermoplastic resin, due to its low impact resistance and long reaction time. Thermoplastic resin softens when heated to or above its glass-transition temperature or to a temperature at or above the melting point, and generally has lower creep strength and heat resistance than thermosetting resin. Another disadvantage is that it is difficult to add a large amount of carbon filler due to its high viscosity. On the other hand, it has the advantages of high toughness and impact resistance. It also enjoys high productivity, since it quickly

solidifies when cooled below its melting point or glass-transition temperature.

Although the characteristics thus differ between the resin types, the common issues are compatibility with regards to conductivity, material strength, and the hydrogen-gas leakage barrier property. The carbon filler must be added in 35 to 85 wt.% to increase conductivity. Although the conductivity increases with the amount of carbon filler added, the strength and hydrogen-gas leakage barrier property decrease due to the aggregation of carbon fillers and void formation caused by the resin not covering the carbon filler completely.[31), 37)] Carbon-resin composite materials are mainly formed into bipolar plate shapes by compression or injection molding; however, a resin-rich layer with low carbon filler composition is formed on the surface, resulting in a significant increase in ICR.[14), 31)] For this reason, several methods have been investigated, including a method to remove the resin-rich layer using Ar plasma or by mechanical polishing,[32), 33)] a method to prevent the formation of a resin-rich layer by inserting a soft film such as fluoride ethylene-propylene copolymer between the carbon-resin composite and the mold during molding,[34)] and a method of forming a graphite film on the surface by inserting graphite foil between the mold and the carbon-resin composite and performing compression molding.[35)] The features of the manufacturing method of carbon-resin composite materials and bipolar plates are summarized by A. Tang et al.,[36)] S. Porstmann et al.,[14)] and N. Saadat et al.,[37)] and these references should be consulted.

### 2.2 Metallic materials

The high strength of metals enables weight reduction by thinning, and channels can be easily formed by press forming. In addition, its high electrical and thermal conductivity and the absence of hydrogen gas leakage problems make it a strong candidate material for bipolar plates in PEMFCs. However, due to the high temperature, high humidity, and acidic corrosive environment inside PEMFCs, metal ions dissolve due to corrosion and penetrate the platinum catalyst layer as well as polyelectrolyte membrane, poisoning them and reducing their output and leading to power generation failure in the worst case.[8), 15)] In addition, the ions of transition metals such as Fe, Co, and Cu act as catalysts for the Fenton reaction, which generates OH radicals that destroy the solid polymer electrolyte membrane in PEMFC.[15), 38)] For this reason, metals such as aluminum,[39), 40)] copper,[41), 42)] stainless steel,[43)-57)] and titanium[58)-68)] have been considered. However, in consideration of corrosion resistance, these have been reduced to corrosion-resistant metals, i.e., stainless steel and titanium.[14)] A Google scholar search of English papers on corrosion resistance and contact resistance for the five years from 2017 to 2021 shows 64 for stainless steel and 23 for titanium, compared with 9 for aluminum and 4 for copper. In particular, stainless steel has been the most widely considered because it has a lower base material cost than titanium. On the other hand, although titanium is more expensive than stainless steel, it shows high corrosion resistance in high temperatures, high humidity, and acidic atmospheres.[8)] Thus, it has less elution as metal ions and less toxicity to solid polymer electrolyte membrane and platinum catalyst.[69)] Furthermore, its low density, approximately 60% of that of stainless steel, contributes to the weight reduction of PEMFC. Stainless steel and titanium exhibit corrosion resistance thanks to an oxide film called passivation film with a thickness of several to 10 nm. However, this film brings high electrical resistance on the surface, resulting in high ICR, low power generation efficiency, and in the worst case, power generation failure. Therefore, the practical application of metallic bipolar plates depends on developing an inexpensive surface treatment technology that combines corrosion resistance and conductivity.

## 3. Surface treatment technology for metallic bipolar plates

Regardless of the type of base material, the surface treatments under consideration are classified as follows: i) nitride[44), 51), 61)] and carbide[63), 64)] films of group 4a, 5a, 6a elements in the periodic table; ii) films of amorphous carbon[49), 53), 68)] and graphene[62), 66)]; iii) conductive oxide films[57)]; iv) films that are diffusion-processed such as chromizing[56)] and nitriding[60)]; v) films of noble metals,[48)] 4a, 5a group metals[70), 71)] or Ni-P plated[65)] metals; and vi) resin films containing conductive nanoparticles.[72)] Except for v) and vi), the films are conventional hard films, most of which are deposited by existing methods. The rest are those in which multilayering of these films attempted to improve adhesion,[43), 54)] pinhole reduction to improve corrosion resistance,[50), 55)] and doping of elements to improve corrosion resistance and ICR.[43), 47), 73)]

**Table 2** and **Table 3** summarize the results of ICR and polarization current measurements before and after the polarization testing for the main surface treatments of stainless steel and titanium over the last five years. The types of films studied

**Table 2** A summary of the results of corrosion tests and ICR measurements of coatings for stainless steel bipolar plates in the main literature in the past 5 years

| Substrate | Coating & film thickness(nm) | Coating method[3] | Corrosion test condition | | | P[1] (MPa) | ICR(mΩ·cm²) | | ΔICR[2] (mΩ·cm²/h) | Corrosion current (μA/cm²) | Ref. |
|---|---|---|---|---|---|---|---|---|---|---|---|
| | | | Electrolyte | Temp. (℃) | Polarization conditions ①anode, ②cathode | | Before polarization | After cathode polarization | | | |
| SUS316L | Ti-doped a-C[3](625-725)/Ti(100) | MS | 0.5M $H_2SO_4$ + 2ppm $F^-$ | 70 | ②0.6VvsSCE for 2h 1.4sSCE for 1h | 1.5 | Coated =3.47－5.64 | — | — | Coated =0.28-0.58 | 43 |
| SUS430 | β-$Nb_2N$(600) | Molten salt | 0.5M $H_2SO_4$ + 2ppm $F^-$ | 70 | 0.17VvsSHE for 500h, $H_2$ purge | 1.4 | SUS430=5.3 Coated=2.3 | SUS430=29.5 Coated=3.8 | SUS430=12.1 Coated=0.75 | SUS430=7 Coated=0.1-0.3 | 44 |
| SUS316L | C doped CrTiN | MS | 0.5M $H_2SO_4$ + 0.2ppm $F^-$ | 70 | 1.1VvsSHE for 2h | 1.4 | SUS316L=276 Coated=4.8 | Coated=7.6 | Coated=1.4 | Coated=0.609 | 47 |
| SUS316L | Au dots on TiN | TiN=MS Au=TS | pH3 $H_2SO_4$ + 0.1ppm $F^-$ | 80 | ②0.67VvsAg/AgCl for 96h, air purge | 1.38 | Coated=1.72 | Coated=5.84 | Coated=0.043 | Coated =0.2±0.04 | 48 |
| SUS316L | a-C(545)/Ti:C /Ti(100) | MS and heat treatment | 0.5M $H_2SO_4$ + 2ppm $F^-$ | 70 | ②0.6VvsSCE for 5h | 1.5 | SUS316L=106.12 Coated=3.31 | SUS316L=163.03 Coated=5.64 | SUS316L=11.4 Coated=0.47 | SUS316L=5.96 Coated=0.1 | 49 |
| SUS316L | TiN/TiAlN multilayer | AIP | 0.5M $H_2SO_4$ + 2ppm $F^-$ | 80 | ①-0.1VvsSCE for 4h, $H_2$ purge ②0.6VvsSCE for 4h, $O_2$ purge | 1.4 | SUS316L=59 Coated=6 | SUS316L=94 Coated=10 | SUS316L=8.8 Coated=1 | Coated= ①0.4,②0.73 | 50 |
| SUS316L | CrN | MS | 0.6M $H_2SO_4$ | 60 | ②0.48VvsSCE for 16h, $O_2$ purge | 1.0 | Coated=8.4 | — | — | Coated=0.1 | 51 |
| SUS304 | $TiB_2$($2\times10^4$) | HEMAA | 0.3M $H_2SO_4$ + 2ppm $F^-$ | 25 | No polarization immersion for 480h | 1.5 | SUS304=50 Coated=19 | SUS304=60 Coated=19 | SUS304=0.021 Coated=0 | — | 52 |
| SUS316L | a-C(200) | MS | 0.5M $H_2SO_4$ + 5ppm $F^-$ | 80 | ②0.6VvsSCE for 12h, air purge | 1.5 | SUS316L=12.60 Coated=2.91 | SUS316L=19.28 Coated=4.06 | SUS316L=0.56 Coated=0.096 | Coated =0.00752 | 53 |
| SUS316L | TiN(1100)/Ti TiAlN(1100 -1300)/TiN/Ti | MS | 0.5M $H_2SO_4$ + 5ppm $F^-$ | 70 | ②0.6VvsSCE for 5h, air purge | 1.4 | TiN=8.3 TiAlN=12.6 | TiN=14.3 TiAlN=22.1 | TiN=1.2 TiAlN=1.9 | TiN≒0.11 TiAlN<0.1 | 54 |
| SUS316L | TiN(50)/Ti(50) multilayer | AIP | 0.5M $H_2SO_4$ + 2ppm $F^-$ | 70 | ②0.6VvsSCE for 1h, $O_2$ purge | 1.4 | SUS316L=150 Coated=11 | SUS316L=276 Coated=18 | SUS316L=126 Coated=7 | SUS316L=0.22 Coated=0.033 | 55 |
| SUS316L | Cr($6\times10^4$) | CH | 0.5M $H_2SO_4$ + 2ppm $F^-$ | 70 | ①-0.1VvsSCE for 4h, $H_2$ purge ②0.6VvsSCE for 4h, $O_2$ purge | 1.4 | SUS316L=105.2 Coated=1.4 | SUS316L=166.7 Coated=4.5 | SUS316L=15.4 Coated=0.78 | Coated 0.14-0.16 | 56 |
| SUS316L | Nb-doped $TiO_2$(700) | Sol-gel | 0.1M $H_2SO_4$ | 80 | ②0.6VvsSCE for 720h, air purge | | SUS316L=58 Coated=38 | SUS316L=70 Coated=41 | SUS316L=0.017 Coated=0.0041 | SUS316L=5 Coated=0.042 | 57 |

1) P=Compaction force of ICR measurement . 2) ΔICR=(ICR before polarization - after cathode polarization)/cathode poralization time

3) a-C=Amorphous carbon, MS=Magnetron Sputtering, TS=Thermal Spray, AIP=Arc Ion Plating, HEMAA=High Energy Micro Arc Alloying CH=Chromising

**Table 3** A summary of the results of corrosion tests and ICR measurements of coatings for titanium bipolar plates in the main literature in the past 5 years

| Coating & film thickness(nm) | Coating method[3] | Corrosion test condition | | | P[1] (MPa) | ICR(mΩ·cm²) | | ΔICR[2] (mΩ·cm²/h) | Corrosion current (μA/cm²) | Ref. |
|---|---|---|---|---|---|---|---|---|---|---|
| | | Electrolyte | Temp. (℃) | Polarization conditions ①anode, ②cathode | | Before polarization | After cathode polarization | | | |
| Ta,N-doped $TiO_2$ | Sol-gel | 0.3MHCl | | No polarization only an immersion of 240h | | Coated=71 | Coated=73 | Coated=0.008 | — | 59 |
| $Ti_2N$(700-2100) | Plasma nitriding | pH3 $H_2SO_4$ and 0.1ppm $F^-$ | 80 | ①-0.1VvsSCE for 4h ②0.6VvsSCE for 4h | 1.5 | Uncoated=12.63 Coated=4.06-5.98 | Uncoated=26.25 Coated=4.94-8.0 | Uncoated=3.4 Coated=0.36 | ①Negative ②0.08 | 60 |
| TiN(1900-2800) | AIP | 0.5M $H_2SO_4$ and 2ppm $F^-$ | 70 | — | 1.4 | Uncoated=35.0 Coated=3.0-3.5 | — | — | — | 61 |
| Graphene oxide (2000) | EPD and heat treatment | 0.5M $H_2SO_4$ and 2ppm $F^-$ | | ①-0.1VvsSCE for 4h, $H_2$ bubble ②0.6VvsSCE for 4h, air bubble | 1.8 | Uncoated=173.62 Coated=3.98 | — | — | ①0.264 ②0.294 | 62 |
| TiC(2000) | DGPSM | 0.5M $H_2SO_4$ and 2ppm $F^-$ | 70 | ①-0.1VvsSCE for 4h, $H_2$ bubble ②0.6VvsSCE for 4h, air bubble | 1.4 | Uncoated=98.1 Coated=7.5 | Uncoated=176.9 Coated=16.9 | Uncoated=19.7 Coated=2.4 | ①-0.27 ②0.17 | 63 |
| NbC(700) | Sputtering | 0.5M $H_2SO_4$ and 3ppm $F^-$ | 75 | ①-0.1VvsSCE for 4h, $H_2$ bubble ②0.6VvsSCE for 4h, air bubble | 1.4 | Uncoated=91.9 Coated=16.6 | Uncoated=180.4 Coated=24.5 | Uncoated=22.1 Coated=2.0 | ①-0.26 ②0.32 | 64 |
| Ni-P including TiN nanoparticles | Electroless plating | 0.5M $H_2SO_4$ and 2ppm $F^-$ | 70 | ①-0.1VvsSCE for 5h, $H_2$ bubble ②0.6VvsSCE for 5h, air bubble | 1.4 | — | Coated=3.5-8.7 | — | ①1.56 ②0.21 | 65 |
| Graphene oxide (2000) | ED and heat treatment | 0.5M $H_2SO_4$ and 2ppm $F^-$ | 70 | ①-0.1VvsSCE for 5h, $H_2$ bubble ②0.6VvsSCE for 5h, air bubble | 1.4 | Coated=about 4 | Coated=about 4 | Coated=0 | ①0.2 ②0.2 | 66 |
| Carbon/PTFE/TiN composite(2300) | Hydrothermal method | 0.5M $H_2SO_4$ and 2ppm $F^-$ | 70 | ①-0.1VvsSCE for 5h, $H_2$ bubble ②0.6VvsSCE for 5h, air bubble | 1.6 | Uncoated=80 Coated=9.5-14 | — | — | ①0.92 ②0.53 | 67 |
| a-C(534-1281) /Ti | MS | 0.5M $H_2SO_4$ and 5ppm $F^-$ | 70 | ②0.6VvsSCE for 2h | 1.5 | Coated=6.52 | — | — | ②0.1 | 68 |

1) P=Compaction force of ICR measurement . 2) ΔICR=(ICR before polarization - after cathode polarization)/cathode poralization time

3) MS=Magnetron Sputtering, AIP=Arc Ion Plating, EPD=Cathodic Electrophoretic Deposition, DGPSM=Double Glow Plasma Surface Modification, ED=Electrodeposition

during that period have not changed significantly compared with those of the five years before that, and the main objective has been to improve the performance of films. In polarization testing, which evaluates the elution of metal ions from bipolar plate materials, i.e., corrosion resistance, the components and composition of the evaluation solutions are mainly evaluated under stricter conditions than those shown in Table 1 for the DOE's 2025 target evaluation conditions. Nevertheless, surface-treated stainless steel and titanium meet the current targets of DOE for corrosion. The corrosion current lower than that of the untreated base material, indicating that the surface treatment is effective in improving corrosion resistance. On the other hand, since there is no provision in DOE's goal to measure the ICR after polarization testing, most of the literature measures only the initial ICR before polarization or measures the ICR after a few hours of polarization in a corrosive environment more severe than DOE's conditions. Selecting films with ICR that is stable in the PEMFC environment for metallic bipolar plates is vital. Hence, to compare the film's stability, a 0.5 kmol/m$^3$ aqueous solution of sulfuric acid containing 0 to 5 ppm of fluorine ions, the most frequent evaluation condition in Tables 2 and 3, was prepared. In this aqueous solution, the ICR increment ΔICR per 1 h was calculated by taking the difference between the ICR after polarization and the ICR before polarization and dividing it by the polarization time for the film polarized at an electric potential of 0.6 VvsSCE. The results are shown in Table 2, Table 3, and **Fig. 2**. Although this is a rough estimation of the trend, ΔICR tends to be large for nitride and carbide and small for the films of amorphous carbon and graphene. The conductive carbon material is used as a resin-carbon composite material with high durability, but it also shows excellent characteristics as a film in terms of ICR stability.

It should be noted that the DOE's durability target for 2025 for an 80 kW class fuel cell vehicle is

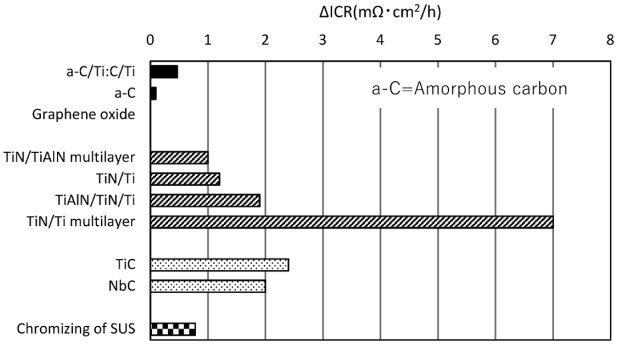


Fig. 2 Amount of increase per hour in ICR of each coating by cathode polarization

set at 8,000 h.[15] To accurately evaluate the durability time of films for metallic bipolar plates, it will be necessary to set appropriate acceleration evaluation conditions and develop evaluation techniques to predict long-term ICR changes.

## 4. Kobe Steel's approach

### 4.1 Kobe Steel's approach to bipolar plate material development

Kobe Steel has been developing surface treatment technology for bipolar plates using titanium as the base material since 2004. Titanium is characterized by its high corrosion resistance and resistance to elution even at high electric potentials. W. Li et al. deposited a film of amorphous carbon on the surface of SUS316L and grade 2 titanium.[68] They observed the surface after 1 h of holding in an aqueous solution at 70℃ of 0.5 kmol/m$^3$ sulfuric acid, with the addition of 2 ppm of fluorine ion, at an electric potential of 1.4 VvsSCE, simulating the start-up and shutdown of a fuel cell vehicle. As a result, they reported that pitting was observed in the pinhole defects of amorphous carbon in SUS316L, while no pitting was observed in titanium. This suggests that titanium is insensitive to elution, even with pinholes. On the other hand, the present author observed cracks in the graphite layer after the press-forming of graphite-coated titanium.[77] E. Haye et al. applied biaxial tension simulating press-forming on a film of CrN deposited on the surface of SUS316L. They reported cracks in the CrN, and approximately 11% of the SUS316L base material was exposed.[51] As mentioned in the previous section, most of the films under consideration are hard, brittle films. Therefore, press forming after surface treatment is considered to cause cracks in the surface-treated layers of both titanium and stainless steel, exposing the base material. However, from the viewpoint of reducing the production cost of bipolar plates, precoat treatment, in which surface treatment is performed before press forming, is advantageous, as pointed out by S. Porstmann et al.[14] and J. M. Huya-Kouadio et al.[26] Precoating can increase productivity by the continuous surface treatment of coils, allowing fuel-cell manufacturers to simply press-form bipolar plates. This eliminates the need for time-consuming handling of each bipolar plate after pressing for transport to the surface treatment process and subsequent surface treatment. Since titanium is corrosion-resistant, pinholes and exposure to the base material are considered acceptable. Thus, it is highly feasible to shorten the film deposition or precoating time, which may result

in thinner films with more pinholes. On the other hand, precoating stainless steel is difficult because the base material exposure increases the risk of degrading power generation performance due to the elution of the base material.

In addition, conventional development has been dominated by using existing film and film deposition technologies to reduce the cost of surface treatment. Against this backdrop, Kobe Steel has been developing unique surface treatment technologies with the goal of precoat titanium, considering that conventional technologies have limitations in performance improvement and production cost reduction. The following is a brief description of surface treatment technologies developed by Kobe Steel.

### 4.2 Titanium material surface-treated with noble metals

Titanium alloy with a mixed film of noble metal and titanium oxide,[74), 75)] and Au-coated titanium with a nano-level thickness of Au film[76)] have been developed using noble metals such as Pd, Pt, and Au, which are resistant to elution in the fuel cell environment and maintain conductivity.

Making a composite coating of noble metal-titanium oxide comprises dissolving titanium by immersing a titanium alloy containing noble metal in a nitric hydrofluoric acid solution to concentrate the noble metal on the surface and performing oxidation treatment in low oxygen partial pressure. The thin film is approximately 50 nm thick, ensuring conductivity by the noble metals. Ti-0.15 wt.% Pd alloy was immersed in an aqueous sulfuric acid solution at 80℃ and pH 2 for 1,000 h. Its ICR was approximately 5 m$\Omega \cdot cm^2$ before and after the immersion with almost no change. The power generation test incorporating the PEMFC showed excellent power generation performance equivalent or superior to that of graphite bipolar plates.[75)]

Since titanium-noble metal alloy contains noble metal in the titanium matrix, unnecessary noble metal that does not contribute to the ICR leads to higher costs. Au-coated titanium is a cost-effective way to reduce costs by eliminating unnecessary noble metals as much as possible. This is pure titanium coated with a 5 to 20 nm thick Au film deposited by sputtering followed by heat treatment in a vacuum. Generally, the film is deposited after removing the passivation film on the titanium surface to ensure the adhesion of the film. The drawbacks are that the passivation film, which provides corrosion resistance to titanium, is removed and that the removal of this film takes a long time. Hence, a film of Au is deposited without removing the passivation film. A part of the oxygen in the passivation film is diffused and absorbed into titanium by vacuum heat treatment, changing it to oxygen-deficient conductive titanium oxide. This increases the conductivity and improves the adhesion of Au by diffusing Au into the titanium oxide layer. The ICR remained at approximately 4 m$\Omega \cdot cm^2$ after 1,000 h of application of 0.65 VvsSCE electric potentials in an aqueous solution of sulfuric acid at 80℃ and pH 2, showing excellent durability. The PEMFC power generation test showed excellent performance equivalent to or better than that of graphite bipolar plates.

### 4.3 Graphite-coated titanium material[77)]

The noble metal-based film in the previous section has the disadvantage of a high production cost due to the high price of noble metal and the time-consuming vacuum process. Hence, graphite-coated titanium has been developed to reduce costs by adopting an atmospheric process without using noble metals. Aqueous paint containing graphite powder is applied to both sides of the titanium foil. The graphite layer is formed by stretching the graphite powder into a film by passing it through a roll press (**Fig. 3**). Finally, a TiC adhesion layer is formed at the interface between the graphite layer and titanium by heat treatment that also serves as strain relief annealing of titanium. The ICR hardly increased and was maintained at approximately 4 m$\Omega \cdot cm^2$ even after applying the electric potential of 0.65 VvsSCE for 1,000 h in an aqueous solution of sulfuric acid at 80℃ and pH 2, exhibiting excellent durability.

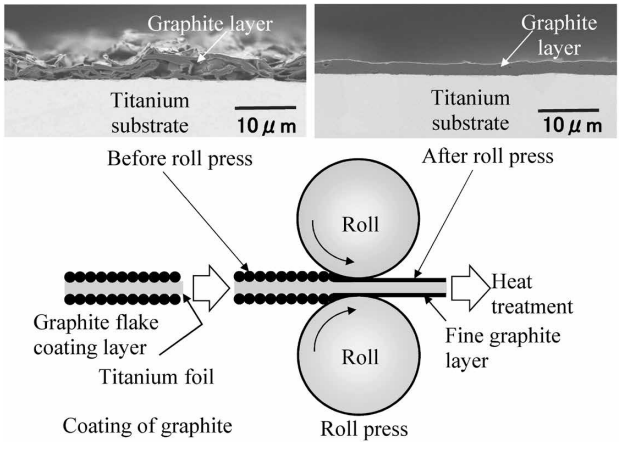


Fig. 3 Process of graphite coating on titanium and structures of graphite layers before and after roll press

## Conclusions

The bipolar plate is a critical component that dramatically affects the performance, life, and cost of PEMFCs. Efforts are underway to improve the performance and reduce the cost of carbon-resin composite material and surface-treated metal, which are candidates for bipolar plate materials. The major challenges in the case of carbon-resin composites are compatibility between the material strength/ hydrogen leakage barrier and bulk resistance/ contact resistance, and in the case of metals, the development of surface treatment film that achieves long-term durability at a low cost. Since titanium can be precoated and has excellent corrosion resistance, it is a promising material with the potential for cost reduction through increased bipolar plate productivity and long-term durability.

Kobe Steel has been developing a unique surface treatment technology for titanium for many years, aiming at durability and cost reduction. As a result, the company has developed precoat type nano-Carbon composite coat (NC) titanium and realized its mass production. NC titanium is used as bipolar plate material in the MIRAI (trademark of Toyota Motor Corporation), a fuel cell vehicle launched in December 2020. Kobe Steel will strive to continue its efforts for further performance improvement and cost reduction and contribute to carbon neutrality through the prevalence of fuel cell vehicles.

## References


1) Ministry of Economy, Trade and Industry. Green Growth Strategy Through Achieving Carbon Neutrality in 2050. 2021.
2) S. Gottesfeld et al. Adv. Electrochem. Sci. Eng. 1997, Vol.5, pp.195-301.
3) Y. Tang et al. Appl. Energy, 2011, Vol.88, pp.68-76.
4) D. Garrain et al. Smart Grid and Renewable Energy. 2011, Vol.2, No.2, Article4954.
5) Y. Tanaka et al. TOYOTA Technical Review. 2021, Vol.66, No.2, pp.6-11.
6) S. Mahabunphachai et al. J. Power Sources. 2010, Vol.195, No.16, pp.5269-5277.
7) T. Kawai. Jour. Jpn. Soc. Mech. Eng. 2016, Vol.119, No.1169, pp.206-211.
8) T. Bohackova et al. Materials. 2021, Vol.14, No.10, Article 2682.
9) S. Karimi et al. Ad. Mater. Sci. Eng. 2012, Article828070.
10) S. Mizuno et al. TOYOTA Technical Review. 2021, Vol.66, No.2, pp.22-27.
11) H. Nakaji et al. Manufacturing & Technology. 2016, Vol.68, No.2, pp.72-75.
12) M. Hashimoto et al. J. Jpn. Inst. Met. 2007, Vol.71, pp.545-552.
13) M. Ueda et al. J. Japan Inst. Met. Mater. 2007, Vol.71, No.7, pp.545-552.
14) S. Porstumann. J. Manufac. Proc. 2020, Vol.60, pp.366-383.
15) U. S. DRIVE Fuel cell technical team roadmap New York US Drive partnership. 2017, pp.1-34.
16) R. Taherian et al. Mater. & Design, 2011, Vol.32, pp.3883-3892.
17) J. H. Lee et al. J Power Sources. 2009, Vol.193, pp.523-529.
18) N. A. M. Radzuan et al. Composition Part B. 2017, Vol.110, pp.153-160.
19) A. Masand et al. Mater. Res. Express. 2017, Vol.4, No.9, Article095604.
20) P. Rzeczkowski et al. Polymers. 2019, Vol.11, No.3, Article 462.
21) K. Yao et al. Energy & Fuels. 2017, Vol.31, No.12, pp.14320-14331.
22) M. Phuangngamphan et al. J. Appl. Polym. Sci. 2019, Vol.136, No.11, Article47183.
23) N. A. M. Radzuan et al. Int. J. Hydrogen Energy. 2019, Vol.48, No.58, pp.30618-30626.
24) N. Afiqah et al. Int. J. Hydrogen Energy, 2017, Vol.42, pp.9262-9273.
25) H. Sakai et al. Journal of Japan Society for Fuzzy Theory and Intelligent Informatics. 2019, Vol.1, No.2, pp.653-661.
26) J. M. Huya-Kouadio et al. Electrocem. Soc. 2018, Vol.83, No.1, pp.93-109.
27) H. E. Lee et al. Composite Structures. 2015, Vol.134, pp.44-51.
28) B. Hu et al. Int. J. Hydro. Energy. 2021, Vol.46, pp.25666-25676.
29) E. Planes et al. Composites Sci. Technol. 2015, Vol.110, pp.17-25.
30) M. C. L. de Oliveira et al. Int. J. Hydro. Energy. 2014, Vol.39, pp.16405-16418.
31) K. I. Jeong et al. Composite Structures. 2021, Vol.262, Article 113617.
32) H. N. Yu et al. Composite structures. 2012, Vol.94, pp.1911-1918.
33) B. Avasarala et al. J. Power Sources. 2009, Vol.188, pp.225-229.
34) D. Lee et al. Composite Structures. 2017, Vol.160, pp.976-982.
35) H. N. Yu et al. J. Power Sources. 2011, Vol.196, pp.9868-9875.
36) A. Tang et al. J. Renew. Sustain. Energy. 2021, Vol.13, No.2, Article022701.
37) N. Saadat et al. Renew. Sustain. Energy Rev. 2021, Vol.138, Article110535.
38) Q. Tang et al. Inter. J. Hydro. Energy. 2021, Vol.46, pp.22040-22061.
39) J. Barranco et al. Inter. J. Hydro. Energy. 2010, Vol.35, pp.11489-11498.
40) A. E. Fetohi et al., Inter. J. Hydro. Energy. 2012, Vol.37, pp.7677-7688.
41) V. V. Nikam et al. Electrochem. Acta. 2006, Vol.51, pp.6338-6345.
42) S.S. Hsieh et al. Micron. 2008, Vol.39, pp.263-268.
43) W. Li et al. Mater. Chem. and Phys. 2022, Vol.276, Article 125234.
44) L.X. Yang et al. Inter. J. Hydrogen Energy. 2021, Vol.46, pp.33206-33214.
45) Q. Jia et al. Mater. Today Chem. 2021, Vol.21, Article100521.
46) J. Li. J. Mater. Sci. 2021, Vol.56, pp.8689-8703.
47) B. Mi et al. Inter. J. Hydrogen Energy. 2021, Vol.46, pp.32645-32654.
48) X. Z. Wang et al. Corrosion Sci. 2021, Vol.189, Article 109624.
49) W. Li et al. Inter. J. Hydrogen Energy. 2021, Vol.46, pp.22983-22997.

50) S. P. Mani et al. J. Mater. Sci. 2021, Vol.56, pp.10575-10596.
51) E. Haye et al. Inter. J. Hydrogen Energy, 2020, Vol.45, pp.15358-15365.
52) R. Y. He et al. Corrosion Science. 2020, Vol.170, Article 108646.
53) H. Li et al. J. Power Source. 2020, Vol.469, Article228269.
54) J. Jin et al. Mater. Chem. and Phys. 2020, Vol.245, Article 122739.
55) S. Jannat et al. J. Power Source. 2019, Vol.435, Article226818.
56) Z. Dong et al. Inter. J. Hydrogen Energy. 2019, Vol.44, pp.22110-22121.
57) Y. Wang et al. Corrosion Sci. 2018, Vol.142, pp.249-257.
58) W. Yan et al. Diamond and related Mater. 2021, Vol.120, Article108628.
59) Y. Wang et al. J. alloys and Compounds. 2021, Vol.879, Article160470.
60) H. Shen, L. Wang. Inter. J. Hydrogen Energy. 2021, Vol.46, pp.11084-11091.
61) T. Li et al. Inter. J. Hydrogen Energy. 2021, Vol.46, pp.31382-31390.
62) Y. Liu et al. Coatings. 2021, Vol.11, Article437.
63) J. Shi et al. Inter. J. Hydrogen Energy. 2020, Vol.45, pp.10050-10058.
64) P. Zhang et al. Surface Coating Technology. 2020, Vol.397, Article126064.
65) C. Ouyang et al. Int. J. Electrochem. Sci. 2020, Vol.15, pp.80-93.
66) J. Wang et al. Inter. J. Hydrogen Energy. 2019, Vol.44, pp.16909-16917.
67) P. Gao et al. Inter. J. Hydrogen Energy. 2018, Vol.43, pp.20947-20958.
68) W. Li et al. Diamond and Related Mater. 2021, Vol.118, Article108503.
69) Y. A. Dobrovol'skii et al. Russian J. General Chem. 2007, Vol.77, No.4, pp.752-765.
70) M.-T. Lin et al. Surface Coatings Technol. 2017, Vol.320. pp.217-225.
71) Y. S. Kim et al. Materials. 2021, Vol.14, No.17, Article4972.
72) Y. Wang et al. Progress in Organic Coatings. 2019, Vol.137, Article105327.
73) J. Jin et al. Inter. J. Hydrogen Energy. 2017, Vol.42, pp.11758-11770.
74) T. Sato et al. R&D Kobe Steel Engineering Reports. 2005, Vol.55, No.3, pp.48-51.
75) T. Sato et al. Ti-2007 Sci. and Technol. Japan Inst. of Mater. 2007, pp.1679-1682.
76) T. Sato et al. R&D Kobe Steel Engineering Reports. 2010, Vol.60, No.2, pp.29-32.
77) T. Sato et al. R&D Kobe Steel Engineering Reports. 2015, Vol.65, No.2, pp.21-24.